TU/e EINDHOVEN UNIVERSITY OF TECHNOLOGY

Lignin oxidation with an organic peroxide and subsequent aromatic ring opening

Citation for published version (APA):
Fernandes, M. R. C., Huang, X., Abbenhuis, H. C. L., & Hensen, E. J. M. (2019). Lignin oxidation with an organic peroxide and subsequent aromatic ring opening. *International Journal of Biological Macromolecules*, *123*, 1044-1051. https://doi.org/10.1016/j.ijbiomac.2018.11.105

DOI:
10.1016/j.ijbiomac.2018.11.105

Document status and date:
Published: 15/02/2019

Document Version:
Publisher's PDF, also known as Version of Record (includes final page, issue and volume numbers)

Please check the document version of this publication:

• A submitted manuscript is the version of the article upon submission and before peer-review. There can be important differences between the submitted version and the official published version of record. People interested in the research are advised to contact the author for the final version of the publication, or visit the DOI to the publisher's website.
• The final author version and the galley proof are versions of the publication after peer review.
• The final published version features the final layout of the paper including the volume, issue and page numbers.

Link to publication

General rights
Copyright and moral rights for the publications made accessible in the public portal are retained by the authors and/or other copyright owners and it is a condition of accessing publications that users recognise and abide by the legal requirements associated with these rights.

• Users may download and print one copy of any publication from the public portal for the purpose of private study or research.
• You may not further distribute the material or use it for any profit-making activity or commercial gain
• You may freely distribute the URL identifying the publication in the public portal.

If the publication is distributed under the terms of Article 25fa of the Dutch Copyright Act, indicated by the "Taverne" license above, please follow below link for the End User Agreement:

www.tue.nl/taverne

Take down policy
If you believe that this document breaches copyright please contact us at:

openaccess@tue.nl

providing details and we will investigate your claim.

Download date: 04. Oct. 2023

International Journal of Biological Macromolecules 123 (2019) 1044–1051

Contents lists available at ScienceDirect

International Journal of Biological Macromolecules

journal homepage: http://www.elsevier.com/locate/ijbiomac

Lignin oxidation with an organic peroxide and subsequent aromatic ring opening

Mónica R.C. Fernandes [a,b], Xiaoming Huang [a], Hendrikus C.L. Abbenhuis [b], Emiel J.M. Hensen [a,*]

[a] Schuit Institute of Catalysis, Laboratory of Inorganic Materials and Catalysis, Eindhoven University of Technology, PO Box 513, 5600 MB Eindhoven, the Netherlands
[b] Hybrid Catalysies B.V., PO Box 513, 5600 MB Eindhoven, the Netherlands

ARTICLE INFO

Article history:
Received 19 September 2018
Received in revised form 18 October 2018
Accepted 12 November 2018
Available online 17 November 2018

Keywords:
Biomass
Lignin
Oxidation
Aromatic ring opening

ABSTRACT

The oxidation of an organosolv lignin with *tert*-butylhydroperoxide, initiated by titanium grafted into the lignin structure, was investigated. Titanation of reactive groups on lignin is responsible for the cross-linking of the lignin structure. IR and MAS ^{13}C NMR spectroscopy spectra confirmed the oxidation of the lignin structure and other pronounced structural changes. A study with guaiacol as a model compound helped to recognise that aromatic ring opening occurs under the given conditions and is catalysed by the grafted titanium. The structure of the oxidised lignin becomes less robust and therefore potentially more susceptible to be depolymerised and converted into monomeric units.

© 2018 The Authors. Published by Elsevier B.V. This is an open access article under the CC BY-NC-ND license (http://creativecommons.org/licenses/by-nc-nd/4.0/).

1. Introduction

Lignin is a natural polymer fundamental to the plant cell walls, together with cellulose and hemi-cellulose. Its main functions are to bring rigidity and contribute to plants structural integrity [1]. Lignin biosynthesis is the result of a radical polymerization of three constituent monomers *p*-coumaryl alcohol, coniferyl alcohol, and sinapyl alcohol, which form respectively the *p*-hydroxyphenyl (H), guaiacyl (G) and syringyl (S) lignin subunits. As this polymerization is a random process, lignin has a high structural diversity [2].

Over the past decades, lignin has been studied as a natural resource in multiple fields. As its structure is rich in aromatic moieties, lignin is a potentially cheap alternative source for the production of bio-based gasoline fuel components and aromatic base fine chemicals [3]. The lingering challenge is to break the recalcitrant lignin structure into aromatic monomers at conversion rates and production distribution that can lead to a commercially viable process. So far, catalytic depolymerization is the most promising approach to achieve this goal [3,4]. Among the many approaches, alcohols such as methanol or ethanol used as supercritical solvents and hydrogen donors represent a new medium and reactant for lignin depolymerisation [5–7]. This and other catalytic approaches remain at the research stage. Another challenge in this respect is associated with the recalcitrant nature of the lignin extracted from the lignocellulosic biomass matrix. Methods for isolating lignin at an industrial scale such as Kraft pulping or organosolv extraction result in a substantial change in the molecular structure of the lignin [8]. The fraction strong in carbon-carbon bonds between the aromatic constituents increases at the expense of the weaker oxygen-containing bonds, primarily weak ether bonds. These changes are the results of repolymerization reactions involving radicals obtained during the isolation step. As a result, ex planta or technical lignins are much more difficult to depolymerize than in planta lignin. Therefore, an approach like the lignin first process presents a novel approach with higher yields of a limited number of aromatic products [9]. This methodology benefits lignin extraction from the wood prior to cellulose. However, the depolymerization of the lignin extracted by this methodology cannot be considered a waste recovery approach, because it does not substantially contribute to the recovery of the 50 million tonnes of lignin isolated per year as industrial waste (mainly form the pulp and paper industry) [10,11].

As a contribution to lignin valorisation, oxidative pre-treatment of lignin has been described as a way to weaken the lignin structure, making it more susceptible to depolymerisation [12]. Several reports mention the oxidation of hydroxyl groups from primary and secondary carbons of the lignin aliphatic chains. The oxidation results in a higher susceptibility of lignin to depolymerisation, achieving higher reaction rates under milder conditions. Stahl and his co-workers explored the use of TEMPO as a catalyst and proposed a mechanism in which a C_α benzylic carbonyl group formed by oxidation can polarize the C_β—H bond, promoting acid-catalysed ether bond cleavage [13,14]. Westwood and co-workers combined C_α oxidation with 2,3-dichloro-5,6-dicyano-1,4-benzoquinone (DDQ) and a zinc catalyst which promotes the C-OAryl bond cleavage [15]. Bolm and co-workers reported a one-pot reaction with a TEMPO

* Corresponding author.
E-mail address: e.j.m.hensen@tue.nl (E.J.M. Hensen).

https://doi.org/10.1016/j.ijbiomac.2018.11.105
0141-8130/© 2018 The Authors. Published by Elsevier B.V. This is an open access article under the CC BY-NC-ND license (http://creativecommons.org/licenses/by-nc-nd/4.0/).

catalyst, which starts with C_γ oxidation followed by a retro-aldol reaction and consequently depolymerisation [16].

In this study, we also explore the oxidation of lignin by using *tert*-butylhydroperoxide (**^{t}BHP**) as the oxidant. **^{t}BHP** is a widely used oxidizing agent for diverse applications and known for its high reactivity towards organic compounds in a mild environment (for instance in the Sharpless epoxidation) [17,18]. As a catalyst, we explored the use of Ti bound to the free hydroxyl groups of the lignin structure. Both the incorporation of Ti and the oxidation of lignin with **^{t}BHP** were accomplished under mild conditions. Guaiacol was used as a model compound to mimic the aromatic moieties in lignin.

2. Materials and methods

2.1. Chemicals and analysis

Organosolv lignin was extracted from beech wood and provided by ECN (now TNO). **^{t}BHP** (70% aqueous solution, Sigma Aldrich) was extracted with n-octane prior to use. Titanium (IV) isopropoxide (**Ti**(**O^{i}Pr**)**$_4$**, Sigma Aldrich) was distilled before use. 2-chloro-4,4,5,5-tetramethyl-1,3,2-dioxaphospholane was synthesized from pinacol and phosphorus trichloride according to a method described in the literature [19]. All other chemicals were obtained from Sigma Aldrich and used as received.

2D Heteronuclear Single Quantum Coherence Nuclear Magnetic Resonance spectroscopy (^{1}H–^{13}C HSQC NMR) spectrum was recorded using a VARIAN INOVA 500 MHz spectrometer equipped with a 5 mm ID AutoX ID PFG Probe. Spectra were obtained using the phase-sensitive gradient-edited HSQC program (gHSQCAD). The main parameters were as follows: 16 scans, acquired from 0 to 16 ppm in F2 (^{1}H) with 1200 data points (acquisition time 150 ms), 0 to 200 ppm in F1 (^{13}C) with a 2 s relaxation delay and 256 t_1 increments (acquisition time 10 ms). The samples were prepared with a concentration of 100 mg of the lignin in 0.6 mL dimethyl sulfoxide-d_6 (DMSO-d_6). Data processing was carried out using the MestReNova software. The central DMSO solvent peak was used as an internal reference (δ_C 39.5, δ_H 2.49 ppm). The cross-peaks were assigned according to the literature [20]. Phosphorus, proton, and carbon (^{31}P, ^{1}H, and ^{13}C) NMR spectra were recorded at 296 K using a Bruker 400 MHz spectrometer. To record quantitative ^{31}P NMR spectra we used a 25 s relaxation delay between 30° pulses, 128 scans and an inverse gated decoupling pulse sequence. The chemical shift was calibrated relative to the internal standard for which the cyclohexanol peak signal centred at δ_P 144.2 ppm was used. Integration regions that were used to assign the signal and relative signal intensities used to calculate the concentration of the hydroxyl group are highlighted in Fig. S2 and Table S1. ^{13}C NMR spectra were recorded with a 1.5 s relaxation delay, 16 scans and 256 time increments. The chemical shift was calibrated relative to the $CDCl_3$ resonance signal centred at δ_C 77.0 ppm. MAS ^{13}C NMR spectra were recorded on a Bruker DMX-500 NMR spectrometer, using a 4 mm zirconia rotor at a spinning rate of 10 kHz and a frequency of 125 MHz. ^{13}C chemical shifts were referenced to adamantine. The acquisition was performed with a standard CP pulse using 2 ms proton 90° pulse, an 800 ms contact pulse and an acquisition time of 20 ms.

X-ray photoelectron spectroscopy (XPS) measurements were carried out on a Thermo Scientific K-Alpha spectrometer equipped with a monochromatic small-spot X-ray source and a 180° double-focusing hemispherical analyser with a 128-channel detector. Spectra were obtained using an aluminium anode (Al K_α = 1486.6 eV) operating at 72 W and a spot size of 400 μm; samples were not handled under an inert atmosphere and should be considered passivated. Survey scans were measured at a constant pass energy of 200 eV and region scans at 50 eV. The background pressure of the UHV chamber was 2×10^{-8} mbar. Compounds were calibrated by setting the C 1s adventitious carbon position to 284.8 eV.

Fourier-transform infrared spectroscopy (FT-IR) spectra were recorded on a Shimadzu MIRacle 10 single reflexion ATR accessory in the 4000–500 cm^{-1} wavelength region.

The metal content was determined by inductively coupled plasma atomic emission spectrometer (ICP-AES) on a Spectro Ciros CCD ICP optical emission spectrometer with axial plasma viewing. All the samples (20 mg) were dissolved in 50 mL aqueous solution with 10 mL of H_2SO_4 and 2 mL of H_2O_2.

2.2. Synthesis of Ti-modified organosolv lignin

Pre-dried organosolv lignin (1.0 g) was dissolved in 50 mL dry ethyl acetate. 5.6 mL **Ti**(**O^{i}Pr**)**$_4$** were added dropwise to this solution. The mixture was kept at room temperature and under argon atmosphere for 2 h (the experiment was carried out in Schlenk). Upon completion, the suspension was dried under vacuum and the solid washed with ethyl acetate to remove traces of unreacted **Ti**(**O^{i}Pr**)**$_4$**. Due to its insoluble character in common solvents, the product (Ti-modified lignin) was characterized by elemental analysis, IR spectroscopy, XPS and MAS ^{13}C NMR.

2.3. Oxidation of Ti-modified lignin with ^{t}BHP

For a typical oxidation reaction, approximately 100 mg of **Ti-lignin** were suspended in 5.0 mL solution of **^{t}BHP** (1.0 M in n-octane). The heterogeneous mixture was stirred (600 rpm) at 60 °C for 24 h. After completion, the product (Oxidised Ti-modified Lignin) was separated by centrifugation, washed with n-octane and dried under vacuum. The product was insoluble and, therefore, it was characterized by IR and MAS ^{13}C NMR spectroscopy.

2.4. Synthesis of Ti-modified guaiacol

Experiments were carried out under inert atmosphere using standard Schlenk techniques. Guaiacol (1.5 g, 11.9 mmol, 1 eq.) was dissolved in 20 mL of ethyl acetate and **Ti**(**O^{i}Pr**)**$_4$** (3.5 mL, 11.9 mmol, 1 eq.) was added dropwise under vigorous stirring. The reaction was kept at these conditions for 2 h. The final mixture was dried under vacuum. The product (Ti-modified Guaiacol 1:1, **Ti-gua**(**1**)) was characterized by ^{1}H NMR, ^{13}C NMR, IR spectroscopy and elemental analysis. Analysis showed that the yellow powder obtained is a mixture of two compounds: $Ti(O^iPr)_3(OC_6H_4OMe)$ and $Ti(O^iPr)_2(OC_6H_4OMe)_2$. As determined by ICP analysis the Ti content was 13.2 wt% of Ti. Experiments were repeated using 4 equivalents of guaiacol instead of 1. The product (Ti-modified Guaiacol 4:1, **Ti-gua**(**4**)) is a mixture of compounds, mainly $Ti(O^iPr)_1(OC_6H_4OMe)_3$ and $Ti(OC_6H_4OMe)_4$.

2.5. Oxidation of Ti-modified guaiacol with a ^{t}BHP solution

An amount of approximately 100 mg of **Ti-gua**(**1**) was dissolved in 5.0 mL solution of **^{t}BHP** in n-octane. There were prepared 9 solutions of **^{t}BHP** with the following oxidant concentrations: 0.02 M, 0.05 M, 0.08 M, 0.10 M, 0.25 M, 0.50 M, 0.75 M, 1.00 M and 2.00 M. The reaction mixture was kept at 60 °C and stirred at 600 rpm for 24 h. The product (oxidised Ti-modified guaiacol, **Oxi-gua**) precipitated during the reaction and was isolated by centrifugation, washed with n-octane to remove traces of side products and dried under vacuum. Due to its insoluble character, **Oxi-gua** was characterized by IR and MAS ^{13}C NMR spectroscopy.

2.6. Derivatization with 2-chloro-4,4,5,5-tetramethyl-1,3,2-dioxaphospholane

A stock solution was made by dissolving 6.2 μL cyclohexanol and 8.4 mg chromium(III)acetylacetonate in 1.5 mL pyridine/$CDCl_3$ (1.6:1; v/v). 13 mg of organosolv lignin was dissolved in 200 μL of pyridine/$CDCl_3$ (1.6:1 v/v) and 400 μL of stock solution was added. Finally, 30 μL

of 2-chloro-4,4,5,5-tetramethyl-1,3,2-dioxaphospholane was added to the prepared lignin solution and stirred to form a homogeneous mixture.

3. Results and discussion

3.1. Lignin characterization

We used an organosolv lignin extracted from beech wood (a hardwood) via the solvent extraction method [21]. NMR spectroscopy was applied to characterize this lignin before modifying it. 2D HSQC NMR spectra of the organosolv lignin are shown in Fig. S1. For identification [20] and quantification [22] of the predominant linkages present in this lignin we followed relevant literature. Two regions of the spectra are of particular interest. The oxygenated side-chain region at δ_C/δ_H: 92–45/2.6–5.6 ppm, represents the carbon-proton cross-peaks of the linkages between lignin building blocks (Fig. S1a). The aromatic region at δ_C/δ_H: 125–100/6.2–7.6 ppm relates to cross-peaks of the different C_9-units (Fig. S1b). The most representative linkages in the lignin are β-O-4, β-β and β-5 bonds (Fig. 1). The α position of β-β (δ_C/δ_H: 85/4.63 ppm) and β-5 (δ_C/δ_H: 87/5.47 ppm) bonds are easily distinguished in these spectra. On the other hand, the assigned resonance signal for the α proton/carbon cross-peak of the β-O-4 linkage is weaker (δ_C/δ_H: 72/4.89 ppm; low intensity). In the aromatic region, the predominant C_9-unit is $S_{2,6}$ at δ_C/δ_H: 104/6.62 ppm. The aromatic cross-peaks of H (δ_C/δ_H: 119/6.78 ppm) and G_2 (δ_C/δ_H: 113/6.77 ppm) units are identified as well. Bond quantification is based on the integration of the C_α cross-peaks and uses the integrated G_2 signal as a reference. The calculations indicate a β-O-4 linkage content of 1.9 per 100 Ar, which is low compared to the β-β content (11.1 per 100 Ar) and the β-5 content (3.5 per 100 Ar). The lignin interlinkage distribution is typical for technical lignin [23] and emphasizes the relatively high content of C—C interlinkages, which leads to a low reactivity of the lignin.

Derivatization of the lignin with 2-chloro-4,4,5,5-tetra-methyl-1,3,2-dioxaphospholane followed by quantitative ^{31}P NMR spectroscopy was employed to quantify the amount of OH groups (see Fig. S2) [24–26]. The aliphatic OH content is 0.95 mmol/g, which is relatively low and is in agreement with the low content of β-O-4 interlinkages. On the other hand, the phenolic OH content of this lignin is relatively high: 2.54 mmol/g of phenolic syringyl groups (δ_P: 144–141.5 ppm) and 1.06 mmol/g of phenolic guaiacyl and demethylated hydroxyl groups (δ_P: 140.5–139.8 ppm). The low number of aliphatic OH and the high content of syringyl groups are in good agreement with the 2D HSQC NMR spectra. The presence of the 4-O-5′ condensed phenolic units resonant signal at δ_P 144.3–142.8 ppm and *p*-hydroxylphenolic groups resonant signal at δ_P 138.6–136.9 ppm was not detected on this lignin.

3.2. Lignin titanation and oxidation

The first attempt to oxidise the lignin was done with a simple and commercially available titanium catalyst: titanium(IV) isopropoxide (**Ti(O^{i}Pr)$_4$**). n-Octane was used as the solvent, because of the stability of the organic peroxide in it. A drawback is that lignin cannot be dissolved in n-octane. The lignin was suspended in n-octane followed by addition of the catalyst and **^{t}BHP**. After 2 h reaction at 60 °C, the IR spectrum of the solid product was compared to that of the parent lignin (Fig. S3). The resulting spectra are similar and, specifically, there is no indication of oxidation. GC analysis of the reaction mixture showed that >90% of the **^{t}BHP** added was converted into **^{t}BuOH**. This indicates that the organic peroxide was decomposed by the Ti catalyst and that the lignin was unaffected. A reason might be that lignin cannot be dissolved in n-octane.

In order to overcome this problem, we explored the grafting of the Ti catalyst to the organosolv lignin, followed by oxidation with **^{t}BHP**. For this, we made use of the relatively high hydroxyl content of the lignin. Given the strong Lewis acidity of **Ti(O^{i}Pr)$_4$**, we did not use a base to catalyse the grafting process. Lignin titanation was done in ethyl acetate by adding **Ti(O^{i}Pr)$_4$** dropwise, which resulted in a brown precipitate. Analysis of the Ti-modified lignin showed that the Ti content was 14.3 wt%. An XPS analysis revealed a (surface) Ti content of 13.5 wt%. As the resulting lignin cannot be dissolved in common solvents, we could not further characterize it using 2D HSQC NMR. Therefore, we turned to IR and MAS ^{13}C NMR spectroscopy to track the changes due to the titanation step.

The IR spectra of the Ti-modified and the parent lignin are shown in (Fig. 2a). Two main differences are observed. A band at 656 cm^{-1} in the Ti-modified lignin is a Ti—O bond stretching vibration, while the decreased intensity of the band at 3410 cm^{-1} indicates the consumption of hydroxyl groups. Also, the band at 1330 cm^{-1} (C—O—H bending vibration (C—O deformation)) has a lower intensity after titanation. The band at 2935 cm^{-1} (CH stretch from aromatic methoxy and side-chain methyl) became more intense, which is likely due to the isopropoxide groups remaining as ligands to Ti. The position of this band is consistent with the C—H vibration of CH_3 groups in **Ti(O^{i}Pr)$_4$**.

The MAS ^{13}C NMR spectrum of the parent lignin contains signals in three main regions, between 50 and 90 ppm due to lignin side-chain carbons, between 95 and 160 ppm due to aromatic carbons and between 165 and 180 ppm due to carbonyl carbons [27,28]. Comparison to the NMR spectrum for the Ti-modified lignin (Fig. 2b) revealed two types of changes. In the regions between 15 and 30 ppm and 70–80 ppm, new peaks are seen, which originate from some the isopropyl groups of **Ti(O^{i}Pr)$_4$** that were not substituted when the Ti was loaded on the lignin. The peaks at 19 and 26 ppm correspond to primary carbons of the isopropyl group (CH_3) and the peaks at 72 and 79 ppm to

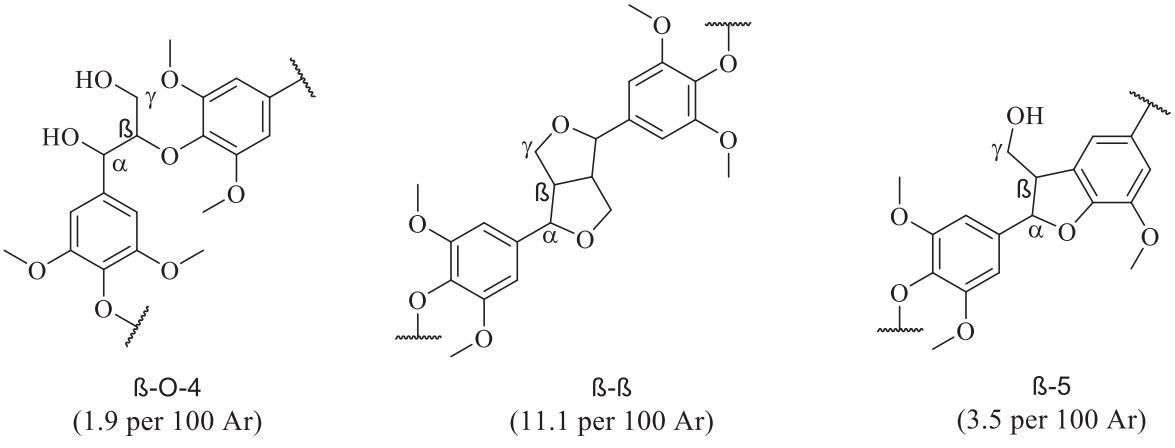

Fig. 1. Chemical structure, identification, and quantification per C_9-unit of the three main linkages find on lignin determined by the ^1H-^{13}C HSQC NMR.

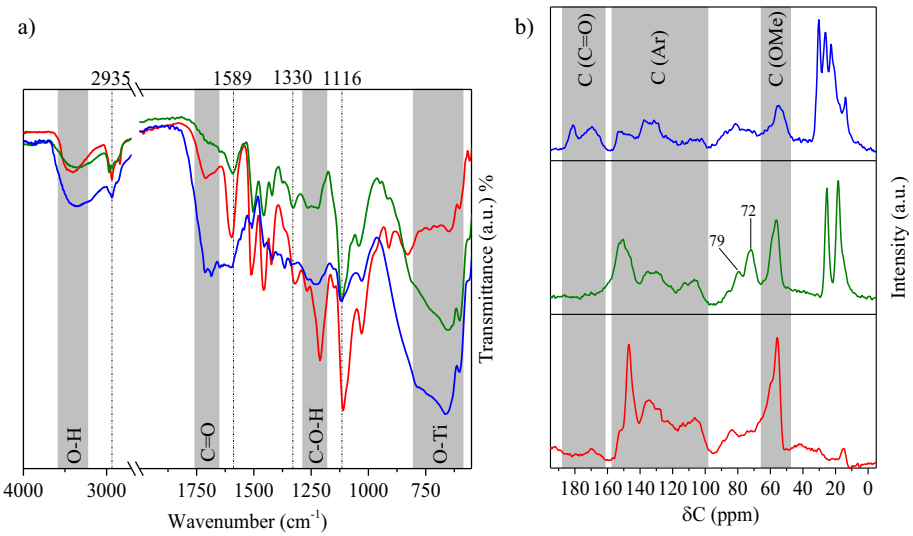

Fig. 2. a) IR and b) MAS ^{13}C NMR spectra of the lignin (red), Ti-modified lignin (green) and oxidised Ti-modified lignin (blue). The main structural changes are highlighted.

tertiary carbons (CH). The fact that there are two peaks for each carbon indicates that there are at least two different types of grafted Ti with different substitution degrees of the parent ligands. The changes registered in the aromatic region were less obvious, but still significant. The ^{13}C NMR signals due to aromatic C can be divided into three groups: the region between 125 and 103 ppm represented non-substituted aromatics; that between 141 and 125 ppm C-substituted aromatic carbons and that from 160 to 141 ppm O-substituted aromatic carbons. There was a small shift of the signal at 128 ppm for the parent lignin to 134 ppm for the Ti-modified counterpart and a significant intensity decrease of the signal at 147 ppm. These changes are the result of the titanium bonding to the phenolic moieties, shifting the signals to a less protected region of the spectrum. The intensity reduction of the signal belonging to the O-substituted aromatic carbons after titanation might be related with the extensive transformation of the phenolic moieties.

As a next step, we explored the **^{t}BHP** oxidation using Ti-modified lignin both as a substrate and as a catalyst. The modified lignin was suspended in a **^{t}BHP** solution in n-octane. After 24 h reaction at 60 °C, the oxidised Ti-modified lignin was isolated and characterized by IR and solid-state NMR spectroscopy, as it remained insoluble in common solvents. The results indicate that lignin lost a large part of its aromaticity. Analysing the IR spectra (Fig. 2a), it is seen that a new band located at 1715 cm^{-1} appears, which is indicative of a larger amount of —C═O stretching vibrations. On the other hand, bands representing the bond stretching vibrations of the aromatic rings became weaker. The characteristic bands of the aromatics at 1116 cm^{-1} (aromatic C—H in-plane deformation), 1421 cm^{-1} (aromatic skeletal vibration combined with C—H deformation), 1503 cm^{-1} (asymmetric aryl ring stretching) and 1589 cm^{-1} (symmetric aryl ring stretching) have lower intensity when compared with the starting Ti-modified lignin. In the ^{13}C NMR spectrum, new peaks located at 169 ppm and 181 ppm confirm the formation of new —C═══O bonds. The region between 180.0 and 168 ppm are the resonance signals of carboxylic acids (—COOH) and esters (—COOR′). Comparing the aromatic rings resonance signals of the titanated with the oxidised lignin, there is a loss of half of the aromatic resonance signals after the oxidation. In conclusion, the main changes are registered in the aromatic ring content and new carbonyl signals point to the lignin oxidation.

3.3. Guaiacol oxidation – a model compound study

We explored the intrinsic chemistry of aromatic ring opening by grafted Ti in more detail using guaiacol as a model compound. This was chosen because the reactions with lignin showed a high titanation degree of phenolic OH groups. The same Ti source (**Ti($O^{i}Pr$)$_4$**) was used to titanate guaiacol. Two Ti-modified guaiacol substrates were synthesized at guaiacol to **Ti($O^{i}Pr$)$_4$** ratios of 1:1 and 4:1. Both were characterized using proton and carbon NMR spectroscopy.

The ^{1}H NMR (Fig. 3a) showed, for both experiments, the disappearance of the guaiacol OH resonance signal at δ_H 5.94 ppm, which is the functional group that grafted to Ti. A shift of the aromatic resonance signals was noticed from δ_H 7.05–6.90 ppm to 6.95–6.60 ppm. The interaction with Ti made the resonance signal of Ar(H) moved to a more protected region of the spectrum. These peaks also become broader and diverse with the increase of guaiacol to Ti ratio, indicating that the product is a mixture of compounds. A new functional group between δ_H 1.29–1.15 ppm is assigned to the resonance signals of the isopropyl groups (CH_3) that were not substituted. The integration of the ^{i}Pr (CH_3) and Ar(H) resonance signals has a ratio of 4 Ar(H) to 12.6 ^{i}Pr (CH_3 protons) for Ti-modified guaiacol 1:1(**Ti-gua**(**1**)) and 4 Ar(H) to 1.5 ^{i}Pr(CH_3 protons) for Ti-modified guaiacol 4:1 (**Ti-gua**(**4**)). This shows that the substitution of O^{i}Pr groups is higher for the **Ti-gua**(**4**).

The ^{13}C NMR spectra (Fig. 3b) clarified the extent of the molecular diversity by the number of aromatic carbons resonance signal located between δ_C 155–100 ppm. In the experiment with an equimolar ratio of guaiacol and **Ti($O^{i}Pr$)$_4$**, the number of aromatic carbons is consistent with a mixture of **Ti($O^{i}Pr$)$_3$(OC_6H_4OMe)** and **Ti($O^{i}Pr$)$_2$(OC_6H_4OMe)$_2$**. On the other hand, the experiment with an excess guaiacol contains a larger number of species. The data suggest that we deal predominantly with **Ti($O^{i}Pr$)(OC_6H_4OMe)$_3$** and **Ti(OC_6H_4OMe)$_4$** (high intensity ^{13}C signals) and traces of guaiacol, **Ti($O^{i}Pr$)$_3$(OC_6H_4OMe)** and **Ti($O^{i}Pr$)$_2$** (**OC_6H_4OMe)$_2$** (Fig. 3d). The same pattern is observed for the ^{13}C resonant signals of the methoxy group between δ_C 57–55 ppm, and it also shows a larger number of signals for the mixture prepared with excess guaiacol. By contrast, the number of isopropyl group ^{13}C resonant signals for the **Ti-gua**(**4**) mixture is lower than for the **Ti-gua**(**1**) sample, specifically considering the CH_3 signal between δ_C 26–25 ppm and the CH signal between δ_C 82–80 ppm. These differences confirm the lower number of isopropyl groups when more guaiacol is added. In fact, it was observed that if we add more guaiacol to a solution of **Ti-gua**(**1**), the substitution of the isopropoxide groups will continue.

The finding that free hydroxyl groups are consumed by substitution of the isopropoxide groups on Ti can explain the low solubility of lignin in common solvents after titanation (like ethyl acetate or THF which previously dissolved it). We suspect that the introduction of Ti as the isopropoxide complex leads to crosslinking of the lignin structure, resulting in a bulkier structure. This could not be tested by GPC due to the insolubility.

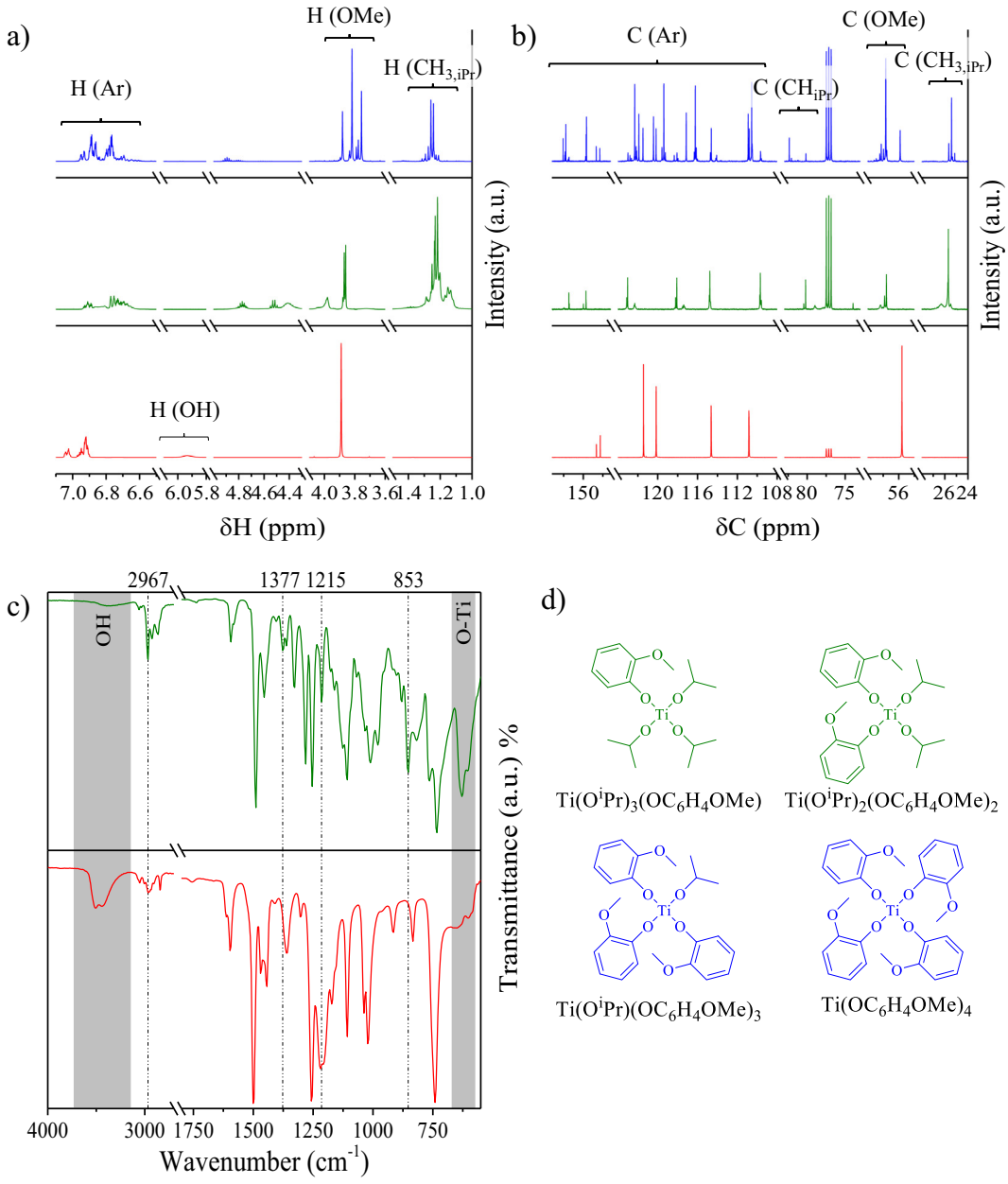

Fig. 3. Comparison between the a) ^{1}H NMR and b) ^{13}C NMR spectra of guaiacol (red), **Ti-gua**(**1**) (green) and **Ti-gua**(**4**) (blue). c) IR spectra of guaiacol (red) and **Ti-gua**(**1**) (green) with the most important bands highlighted identifying the structural changes. d) Chemical structures of **Ti-gua** that were formed in the guaiacol titanation reactions.

We carried out guaiacol oxidation using the **Ti-gua**(**1**), because, due to the higher amount of isopropyl groups, this model compound is a better representative of Ti-modified lignin. The oxidation of the **Ti-gua** (**1**) was evaluated in solutions containing different concentrations of **^{t}BHP** (reaction at 60 °C for 24 h). The products are insoluble in common solvents, similar to the oxidised Ti-modified lignin, and were therefore characterized by IR and MAS ^{13}C NMR spectroscopy.

The IR spectra of **Ti-gua**(**1**) and the guaiacol are shown in Fig. 3c. The differences between these spectra are the appearance of the band at 629 cm^{-1} (Ti—O stretching vibration), the disappearance of the band at 3410 cm^{-1} (OH stretching vibration) and the intensifying of the bands at 2859 cm^{-1}, 2924 cm^{-1}, and 2967 cm^{-1} (stretch vibrations of CH bonds of the isopropyl groups). For the aromatic stretching region, we found that the band at 853 cm^{-1} (Ar C—H out-of-plan deformation vibration) became more intense, while the bands at 1215 and 1377 cm^{-1} (C—O—H bending vibration and C—O stretching vibrations, respectively) became weaker. These changes match the expected results for the grafting of Ti through the guaiacol OH group.

The IR spectra of the products after oxidation with **^{t}BHP** (**Oxi-gua**) are presented in Fig. 4a (respective **^{t}BHP** concentration used to treat the sample is highlighted on the graphic). With increasing oxidant concentration, the structure of the reactant was more affected. The bands at 853 cm^{-1} and 735 cm^{-1} (C—H out-of-plane deformation vibrations), at 1255 cm^{-1} and 1107 cm^{-1} (C—H in-plan deformation vibrations), and at 1490 cm^{-1} and 1592 cm^{-1} (—C=C— stretch vibration) are disappearing with the increase of the **^{t}BHP** concentration. A new band at 1736 cm^{-1} appeared and it is due to new —C=O stretching vibration of unconjugated carboxyl acids. This new band is a clear indication that the reactant was oxidised as expected.

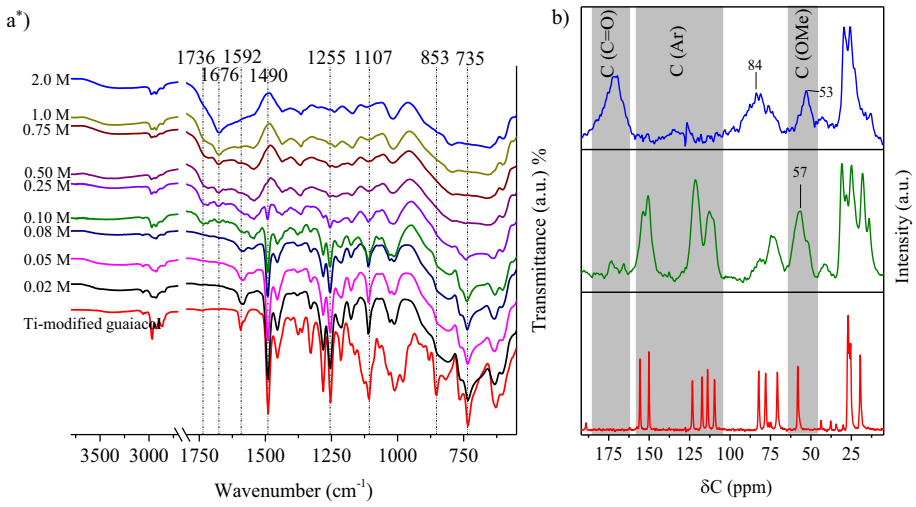

Fig. 4. a) IR spectra of the **Ti-gua**(**1**) after oxidation with different concentrations of **^{t}BHP** and respective b) MAS ^{13}C NMR spectra of guaiacol (red), **Oxi-gua** after oxidation with 0.10 M (green) and 2.0 M (blue) of **^{t}BHP**. The most important signals, identifying the changes with the increase of the oxidation, are highlighted. *The spectra were stacked for clearance.

Oxi-gua samples treated with a low concentration of **^{t}BHP** (0.1 M) and with a higher oxidant concentration (2.0 M) were analysed by MAS ^{13}C NMR (Fig. 4b). In comparison with the **Ti-gua**(**1**), the product treated with less **^{t}BHP** displays minor changes of its structure with the exception of two new peaks appearing at 166 ppm and 173 ppm reflecting the formation of new carbonyl moieties. At higher **^{t}BHP**

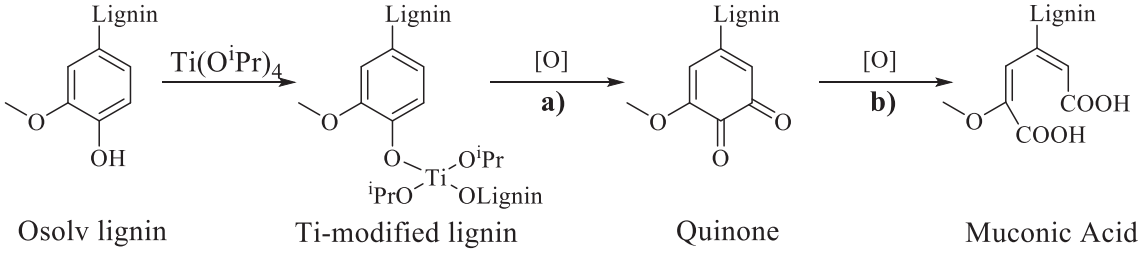

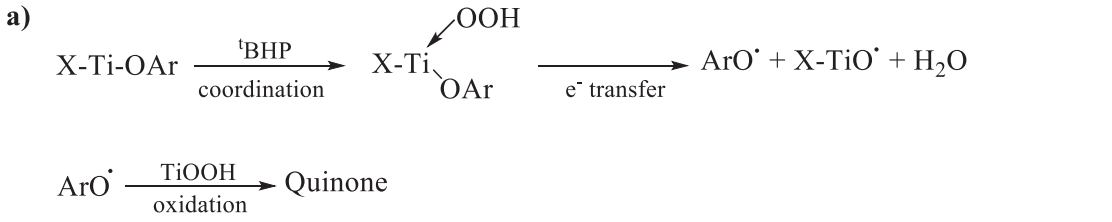

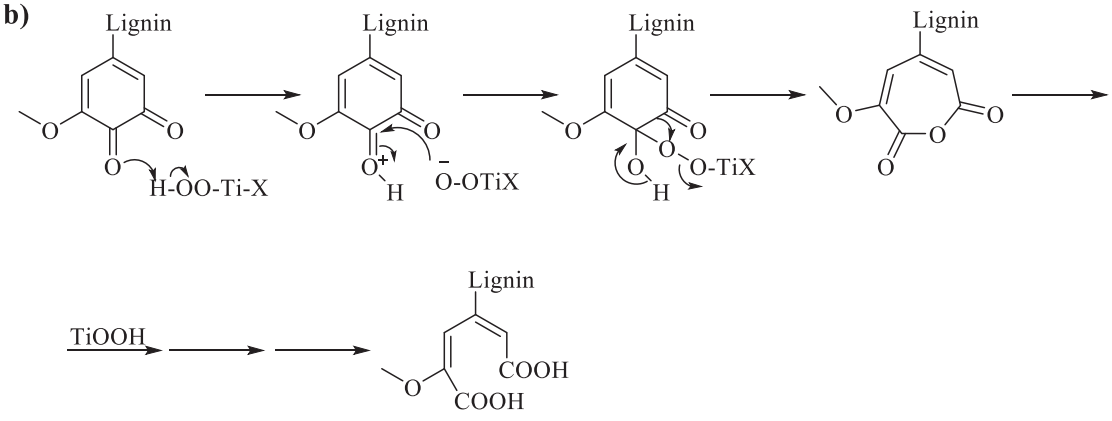

Fig. 5. Reaction pathway of the aromatic ring opening in a typical oxidation with peroxides resulting in the formation of a) quinone and b) muconic acid species thereof [2,32–34].

concentration, the changes are more pronounced. The peaks corresponding to the aromatic C resonant signals disappeared and new ones appeared at 84 ppm (alkene C resonant region) and at 172 ppm. The shift of the C from the methoxyl group resonant signal from 57 ppm to 53 ppm is consistent with the structural change from MeO—Ph to MeO—CH═C—.

These dramatic changes in the aromatic region of the titanated materials (lignin and guaiacol) upon oxidation indicate that aromatic ring opening occurred. The MAS ^{13}C NMR and IR spectra of the oxidised materials demonstrate similar structural changes: new carbonyl group signals and less intense aromatic signals. The partial ring cleavage by oxidation with **^{t}BHP** evidenced is associated with the Ti grafting on the lignin. In all our blank experiments and in an attempt of oxidizing lignin with **Ti($O^{i}Pr$)$_4$** reported initially, there was no indication that the aromatic content of lignin was affected by the oxidant. This extensive structural modification of lignin was already described in the literature as a degradation effect caused by using, for example, H_2O_2, organic peroxides and peracids [2]. Gellerstedt and Agnemo reported that ring opening was found exclusively in the presence of a catalytic metal able to interact with lignin [29]. Another work reported reactions introducing a similar effect on lignin that were promoted by elaborated catalyst like porphyrin-based ones [30,31]. On their studies, the reaction mechanism proposes that the ring opens forming a muconic acid species. In a typical ring-opening reaction by oxidation forming this species, a quinone intermediate is formed as indicated in Fig. 5 [2,32].

The typical ^{13}C NMR resonant signal of quinones lies around δ_C 180 ppm (carbonyl groups in adjacent carbons) and its IR band is located between 1690 and 1675 cm^{-1}. The oxidised Ti-modified lignin MAS ^{13}C NMR spectrum has a peak at δ_C 181 ppm and its IR spectrum has a band at 1680 cm^{-1} which might be an indication of an intermediate stage prior to ring opening. The C resonant signal at δ_C 169 ppm and the IR band at 1736 cm^{-1} represent the carbonyl group from the muconic acids species having their signals in the carboxylic acids regions assigned to lignin.

4. Conclusions

We demonstrated a lignin oxidation process achieved with **^{t}BHP** and using an uncommon method. Grafting titanium to lignin hydroxyl groups was the solution to successfully catalyse the oxidation. Unexpectedly, this method also led to a partial cleavage of the aromatic rings turning the lignin structure less robust what might led to a better depolymerization results to be tested in a future work. The mild conditions employed can be an advantage to an industrial application.

Conflict of interest

The authors declare no conflict of interest.

Acknowledgments

This work was supported by the European Union (Marie Curie ITN 'SuBiCat' PITN-GA-2013-607044).

Appendix A. Supplementary data

Supplementary data to this article can be found online at https://doi.org/10.1016/j.ijbiomac.2018.11.105.

References

[1] A. Kärkönen, S. Koutaniemi, Lignin biosynthesis studies in plant tissue cultures, J. Integr. Plant Biol. (2010)https://doi.org/10.1111/j.1744-7909.2010.00913.x.
[2] C. Heitner, D. Dimmel, J. Schmidt, Lignin and Lignans: Advances in Chemistry, 2010https://doi.org/10.1016/0076-6879(88)61028-7.
[3] J. Zakzeski, P.C.A. Bruijnincx, A.L. Jongerius, B.M. Weckhuysen, The catalytic valorization of lignin for the production of renewable chemicals, Chem. Rev. (2010)https://doi.org/10.1021/cr900354u.
[4] Z. Sun, G. Bottari, A. Afanasenko, M.C.A. Stuart, P.J. Deuss, B. Fridrich, K. Barta, Complete lignocellulose conversion with integrated catalyst recycling yielding valuable aromatics and fuels, Nat. Catal. (2018)https://doi.org/10.1038/s41929-017-0007-z.
[5] X. Huang, T.I. Korányi, M.D. Boot, E.J.M. Hensen, Catalytic depolymerization of lignin in supercritical ethanol, ChemSusChem (2014)https://doi.org/10.1002/cssc.201402094.
[6] X. Huang, T.I. Korányi, M.D. Boot, E.J.M. Hensen, Ethanol as capping agent and formaldehyde scavenger for efficient depolymerization of lignin to aromatics, Green Chem. (2015)https://doi.org/10.1039/c5gc01120e.
[7] S. Gillet, M. Aguedo, L. Petitjean, A.R.C. Morais, A.M. Da Costa Lopes, R.M. Łukasik, P.T. Anastas, Lignin transformations for high value applications: towards targeted modifications using green chemistry, Green Chem. (2017)https://doi.org/10.1039/c7gc01479a.
[8] C. Li, X. Zhao, A. Wang, G.W. Huber, T. Zhang, Catalytic transformation of lignin for the production of chemicals and fuels, Chem. Rev. (2015)https://doi.org/10.1021/acs.chemrev.5b00155.
[9] W.J. Sagues, H. Bao, J.L. Nemenyi, Z. Tong, Lignin-first approach to biorefining: utilizing Fenton's reagent and supercritical ethanol for the production of phenolics and sugars, ACS Sustain. Chem. Eng. (2018)https://doi.org/10.1021/acssuschemeng.7b04500.
[10] Z. Strassberger, S. Tanase, G. Rothenberg, The pros and cons of lignin valorisation in an integrated biorefinery, RSC Adv. 4 (2014) 25310–25318, https://doi.org/10.1039/C4RA04747H.
[11] A.A. Klyosov, G.P. Philippidis, Y.A. Monovoukas, Method of recovering lignin from pulp and paper sludge, US5777086A, 1998.
[12] P.C.A. Bruijnincx, B.M. Weckhuysen, Biomass conversion: lignin up for break-down, Nat. Chem. (2014)https://doi.org/10.1038/nchem.2120.
[13] A. Rahimi, A. Azarpira, H. Kim, J. Ralph, S.S. Stahl, Chemoselective metal-free aerobic alcohol oxidation in lignin, J. Am. Chem. Soc. (2013)https://doi.org/10.1021/ja401793n.
[14] A. Rahimi, A. Ulbrich, J.J. Coon, S.S. Stahl, Formic-acid-induced depolymerization of oxidized lignin to aromatics, Nature (2014)https://doi.org/10.1038/nature13867.
[15] C.S. Lancefield, O.S. Ojo, F. Tran, N.J. Westwood, Isolation of functionalized phenolic monomers through selective oxidation and CO bond cleavage of the β-O-4 linkages in lignin, Angew. Chem. Int. Ed. (2015)https://doi.org/10.1002/anie.201409408.
[16] S. Dabral, J.G. Hernández, P.C.J. Kamer, C. Bolm, Organocatalytic Chemoselective primary alcohol oxidation and subsequent cleavage of lignin model compounds and lignin, ChemSusChem (2017)https://doi.org/10.1002/cssc.201700703.
[17] S. Krijnen, H.C.L. Abbenhuis, R.W.J.M. Hanssen, J.H.C. van Hooff, R.A. van Santen, Solid-phase immobilization of a new epoxidation catalyst, Angew. Chem. Int. Ed. 37 (1998) 356–358, https://doi.org/10.1002/(SICI)1521-3773(19980216)37:3<356::AID-ANIE356>3.0.CO;2-5.
[18] T. Katsuki, K.B. Sharpless, The first practical method for asymmetric epoxidation, J. Am. Chem. Soc. (1980)https://doi.org/10.1021/ja00538a077.
[19] A. Zwierzak, Cyclic organophosphorus compounds. I. Synthesis and infrared spectral studies of cyclic hydrogen phosphites and thiophosphites, Can. J. Chem. 45 (1967) 2501–2512, https://doi.org/10.1139/v67-411.
[20] T.Q. Yuan, S.N. Sun, F. Xu, R.C. Sun, Characterization of lignin structures and lignin-carbohydrate complex (LCC) linkages by quantitative13C and 2D HSQC NMR spectroscopy, J. Agric. Food Chem. (2011)https://doi.org/10.1021/jf2031549.
[21] J. Wildschut, A.T. Smit, J.H. Reith, W.J.J. Huijgen, Ethanol-based organosolv fractionation of wheat straw for the production of lignin and enzymatically digestible cellulose, Bioresour. Technol. (2013)https://doi.org/10.1016/j.biortech.2012.10.050.
[22] F. Tran, C.S. Lancefield, P.C.J. Kamer, T. Lebl, N.J. Westwood, Selective modification of the β-β linkage in DDQ-treated Kraft lignin analysed by 2D NMR spectroscopy, Green Chem. (2015)https://doi.org/10.1039/c4gc01012d.
[23] S. Constant, H.L.J. Wienk, A.E. Frissen, P. De Peinder, R. Boelens, D.S. Van Es, R.J.H. Grisel, B.M. Weckhuysen, W.J.J. Huijgen, R.J.A. Gosselink, P.C.A. Bruijnincx, New insights into the structure and composition of technical lignins: a comparative characterisation study, Green Chem. (2016)https://doi.org/10.1039/c5gc03043a.
[24] D.S. Argyropoulos, H.I. Bolker, C. Heitner, Y. Archipov, 31P NMR spectroscopy in wood chemistry. Part V. Qualitative analysis of lignin functional groups, J. Wood Chem. Technol. (1993)https://doi.org/10.1080/02773819308020514.
[25] D.S. Argyropoulos, Quantitative phosphorus-31 nmr analysis of lignins, a new tool for the lignin chemist, J. Wood Chem. Technol. (1994)https://doi.org/10.1080/02773819408003085.
[26] M. Balakshin, E. Capanema, On the quantification of lignin hydroxyl groups with ^{31}P and ^{13}C NMR spectroscopy, J. Wood Chem. Technol. (2015)https://doi.org/10.1080/02773813.2014.928328.
[27] A. Barapatre, K.R. Aadil, B.N. Tiwary, H. Jha, In vitro antioxidant and antidiabetic activities of biomodified lignin from *Acacia nilotica* wood, Int. J. Biol. Macromol. (2015) https://doi.org/10.1016/j.ijbiomac.2015.01.012.
[28] I. Santoni, E. Callone, A. Sandak, J. Sandak, S. Dirè, Solid state NMR and IR characterization of wood polymer structure in relation to tree provenance, Carbohydr. Polym. (2015)https://doi.org/10.1016/j.carbpol.2014.10.057.
[29] R. Agnemo, G. Gellerstedt, J.J. Leban, U. Björkroth, S. Rosell, K. Folkers, N. Yanaihara, C. Yanaihara, The reactions of lignin with alkaline hydrogen peroxide. Part II. Factors influencing the decomposition of phenolic structures, Acta Chem. Scand. 33b (1979) 337–342, https://doi.org/10.3891/acta.chem.scand.33b-0337.
[30] F. Cui, T. Wijesekera, D. Dolphin, R. Farrell, P. Skerker, Biomimetic degradation of lignin, J. Biotechnol. (1993)https://doi.org/10.1016/0168-1656(93)90023-G.

[31] B. Kurek, I. Artaud, B. Pollet, C. Lapierre, B. Monties, Oxidative degradation of in situ and isolated spruce lignins by water-soluble hydrogen peroxide resistant pentafluorophenylporphyrin, J. Agric. Food Chem. (1996)https://doi.org/10.1021/jf950612g.

[32] J.F. Kadla, H. Chang, The reactions of peroxides with lignin and lignin model compounds, Oxidative Delignification Chem. (2001)https://doi.org/10.1021/bk-2001-0785.ch006.

[33] T.A. Trubitsyna, O.A. Kholdeeva, Kinetics and mechanism of the oxidation of 2,3,6-trimethylphenol with hydrogen peroxide in the presence of Ti-monosubstituted polyoxometalates, Kinet. Catal. 49 (2008) 371–378, https://doi.org/10.1134/S0023158408030087.

[34] G.-J. ten Brink, I.W.C.E. Arends, R.A. Sheldon, The Baeyer—Villiger reaction: new developments toward greener procedures, Chem. Rev. 104 (2004) 4105–4124, https://doi.org/10.1021/cr030011l.